RSC Advances

PAPER

View Article Online
View Journal | View Issue

Cite this: *RSC Adv.*, 2023, **13**, 30771

Highly sensitive and selective detection of triphosgene with a 2-(2′-hydroxyphenyl) benzimidazole derived fluorescent probe†

Wen-Zhu Bi, *[ab] Yang Geng,[c] Wen-Jie Zhang,[a] Chen-Yu Li,[a] Chu-Sen Ni,[a] Qiu-Juan Ma, *[ab] Su-Xiang Feng,*[bde] Xiao-Lan Chen [f] and Ling-Bo Qu[f]

Received 6th September 2023
Accepted 12th October 2023

DOI: 10.1039/d3ra06061f

rsc.li/rsc-advances

In this work, a 2-(2′-hydroxyphenyl)benzimidazole derived fluorescent probe, 2-(2′-hydroxy-4′-aminophenyl)benzimidazole (**4-AHBI**), was synthesized and its fluorescent behavior toward triphosgene were evaluated. The results showed that **4-AHBI** exhibited high sensitivity (limit of detection, 0.08 nM) and excellent selectivity for triphosgene over other acyl chlorides including phosgene in CH_2Cl_2 solution. Moreover, **4-AHBI** loaded test strips were prepared for the practical sensing of triphosgene.

Introduction

As an excellent acylation reagent, triphosgene (bis(trichloromethyl) carbonate (BTC)), also called solid phosgene, is extensively employed as basic chemical raw material for the industrial synthesis of medicines, pesticides, spices, dyes and polymer materials.[1] Besides, triphosgene is also used as a versatile reagent in the development of modern organic synthesis strategy.[2] Compared with traditional acylation reagents (*e.g.* sulfoxide chloride, phosphorus oxychloride, phosphorus trichloride and phosphorus pentachloride), triphosgene presents numerous merits, including low toxic, stable solid with minimal vapour pressure, accurate measurement, mild reaction conditions, high selectivity and reliability, low cost, handy storage and transportation.[3] Despite these huge advantages, the daily use and measurement of triphosgene still needs to be performed under standard safety protocols. The reason behind this is the easy release of highly toxic phosgene gas in the potential presence of nucleophiles (*e.g.* chloride ions, tertiary amines) and the inhalation of phosgene can result to serious and sustained respiratory distress.[4] Therefore, efficient and reliable method for the sensitive detection and identification of triphosgene is specially urgent to protect public health and security from the accidental leakage in industrial accidents.

Compared with conventional gas/liquid chromatography[5] and electrochemical methods[6] with high cost and complicated sample preparation, fluorescent detection methods are well developed and widespread due to their low cost, easy operation and high sensitivity and selectivity.[7] In the past decades, numerous fluorescent probes have been reported for the detection of phosgene.[8] However, most of them give slow or no fluorescence response to triphosgene due to the lower electrophilic property of triphosgene.[9] In 2018 and 2019, Song's group reported two 1,8-naphthalimide derived probe (Phos-2 and Phos-4) for the fluorescent detection of triphosgene through acylation of the amino group based on intramolecular charge-transfer (ICT) mechanism.[10,11] In 2022, Zhou's group disclosed a rhodamine derived fluorescent probe (RDM-670) for visual detection of triphosgene through twice carbamylation reaction.[12] Very recently, Kaur's group reported another 1,8-naphthalimide derived Schiff base (Probe 1) with hydroxyl and amino groups as nucleophilic sites for the fluorescent detection of triphosgene.[13] However, these fluorescent probes still suffer from some drawbacks, such as tedious preparation process, easily disturbed by other acetylating agents and relatively lower sensitivity.

In 2021, we developed an excited-state intramolecular proton transfer (ESIPT)-based fluorescence probe (P1) for the discrimination between phosgene and triphosgene by simple introducing a strong electron-donating amino group at the C5′ position of 2-(2′-hydroxyphenyl)benzimidazole (HBI).[14] Compared with unsubstituted HBI, P1 displayed excellent selectivity for phosgene over triphosgene. For further exploration of the effect of amino group position on the sensing properties and the aim to develop '6S' (simpleness, speedy,

[a]*School of Pharmacy, Henan University of Chinese Medicine, Zhengzhou, China, 450046. E-mail: biwenzhu2018@hactcm.edu.cn; maqiujuan104@126.com*

[b]*Henan Engineering Research Center of Modern Chinese Medicine Research, Development and Application, Zhengzhou, China, 450046. E-mail: fengsx221@163.com*

[c]*Department of Pharmacy, Zhengzhou Railway Vocational and Technical College, Zhengzhou, 450046, China*

[d]*Academy of Chinese Medical Sciences, Henan University of Chinese Medicine, Zhengzhou, 450046, China*

[e]*Collaborative Innovation Center for Chinese Medicine and Respiratory Diseases co-constructed by Henan Province & Education Ministry of P. R. China, Zhengzhou, 450046, China*

[f]*College of Chemistry, Zhengzhou University, Zhengzhou, 450052, China*

† Electronic supplementary information (ESI) available. See DOI: https://doi.org/10.1039/d3ra06061f

selectivity, sensitivity, stability and smart) fluorescence probe, we synthesized another HBI derived probe (**4-AHBI**) through changing the amino group from the C5′ to C4′ position (Scheme 1). To our surprise, preliminary experiments to optimize the amount of triethylamine (TEA) for the generation of phosgene showed a decreased fluorescence intensity @386 nm of **4-AHBI** solution with triphosgene (3.5 μM) upon addition of triethylamine (TEA, 0–1 μM) (Fig. S1†). This result indicated **4-AHBI** would be a competitive fluorescent triphosgene probe.[11,12] The different detection performance of P1 and **4-AHBI** might result from the different electron density during photo-excitation process, which changes the acid–base properties of proton donor and acceptor groups.[15] Compared with previously reported probes for detection of triphosgene, the prominent advantages of this methodology include simple structure, higher sensitivity (limit of detection, 0.08 nM) over the range of 0–0.5 μM and selectivity for triphosgene over other acyl chlorides including phosgene. Furthermore, easily prepared **4-AHBI** loaded test papers were fabricated and display an obvious turn-on fluorescence emission upon treated with triphosgene.

Experimental section

Materials and instruments

All reagents and solvents were obtained from commercial suppliers and used without further purification. ^{1}H and ^{13}C NMR spectra were recorded on a Bruker 400 spectrometer in DMSO-d6 containing tetramethylsilane (TMS) as an internal standard. Fluorescence emission spectra were collected by Hitachi F7000 fluorescence spectrometer (slit width = 2.5/2.5 nm). UV-vis absorption spectroscopy measurements were performed on Thermo Evolution 260 Bio at room temperature. High-resolution mass spectra (HRMS) were obtained on Agilent Technologies 6530 Accurate mass Q-TOF LC/MS with ESI as ion source. Elemental analysis was performed on a Vario PYRO cube Elemental Analyser.

Synthesis of 4-AHBI

4-Aminosalicylic acid (0.15 g, 1.0 mmol) and *o*-phenylenediamine (0.11 g, 1.0 mmol) were mixed and stirred in polyphosphoric acid (85% phosphorus pentoxide, 15 mL) at 160 °C over a period of 6 h.[16] Then the reaction mixture was cooled to room temperature and diluted by saturated $NaHCO_3$ aqueous solution to pH 8–9. The precipitation were collected and further purified by column chromatography (ethyl acetate: petroleum ether = 2 : 1) to give **4-AHBI** (0.11 g, yield 50%) as a brown solid. ^{1}H NMR (400 MHz, DMSO-d6) δ (ppm): 12.97 (br, 1H, NH), 12.67 (br, 1H, OH), 7.66 (d, J = 8.8 Hz, 1H, Ar–H), 7.52 (s, 2H, Ar–H), 7.19–7.17 (m, 2H, Ar–H), 6.23–6.21 (m, 1H, Ar–H), 6.14 (d, J = 2.0 Hz, 1H, Ar–H), 5.66 (s, 2H, NH_2). ^{13}C NMR (100 MHz, DMSO-d6) δ (ppm): 160.29, 153.69, 152.97, 127.55, 122.38, 106.59, 101.37, 100.57. HRMS: $[M + H]^+$: calcd for $C_{13}H_{12}N_3O$: 226.0975, found: 226.0975. Anal. calcd for $C_{13}H_{11}N_3O$: C 69.32, H 4.92, N 18.66; found C 69.51, H 4.89, N 18.73.

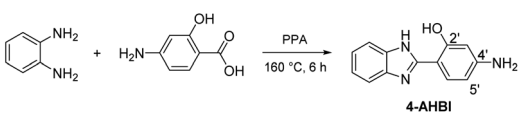

Scheme 1 Synthesis of **4-AHBI**.

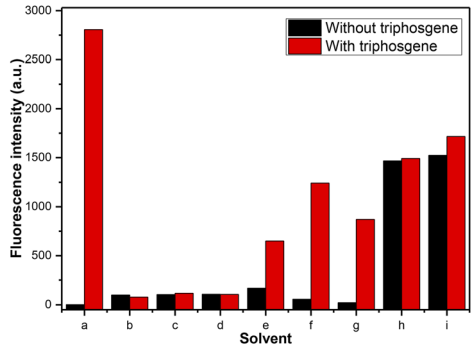

Fig. 1 Fluorescence intensity of **4-AHBI** (10 μM) in different solvents without (black) and with (red) triphosgene (3.5 μM). a: CH_2Cl_2; b: $CHCl_3$; c: MeOH; d: EtOH; e: MeCN; f: acetone; g: EtOAc; h: DMF; i: DMSO.

Analytical procedure

4-AHBI stock solution (1.0 mM, 10 mL) was prepared in CH_2Cl_2 (containing 0.5 mL of DMSO) in a 10 mL volumetric flask for UV-vis and fluorescence titrations. The stock solutions of triphosgene (0.1 mM) and relevant analytes ($(COCl)_2$, CH_3COCl, $SOCl_2$, TsCl, DCP, HOAc, $POCl_3$, SO_2Cl_2, and HCl) (5 mM) were also prepared in CH_2Cl_2. Phosgene were prepared by mixing triphosgene (1.67 mM in CH_2Cl_2) and triethylamine (0.1 mM in CH_2Cl_2). The test solutions were prepared by dilution of the stock solutions. For detection of triphosgene in solutions: 20 μL **4-AHBI** stock solution (1.0 mM) was added in 2.0 mL of CH_2Cl_2 in a 5 mL centrifuge tube, then triphosgene stock solution (0–100 μL) was added. Similar procedure were employed for detection of relevant analytes. All solutions were kept for 30 min before the UV-vis and fluorescence testing.

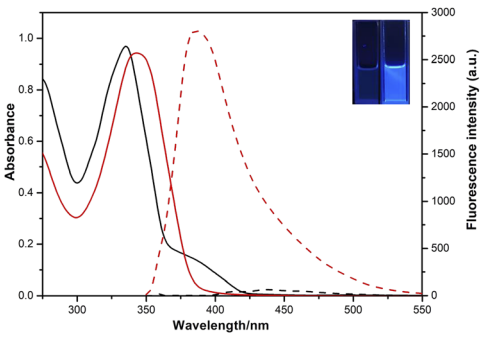

Fig. 2 UV-vis absorption (solid) and fluorescence (dash) spectra of 10 μM **4-AHBI** (black) and the mixture of **4-AHBI** and 3.5 μM triphosgene (red) in CH_2Cl_2. Inset: photograph of **4-AHBI** (left) and the mixture under 365 nm UV-light (right).

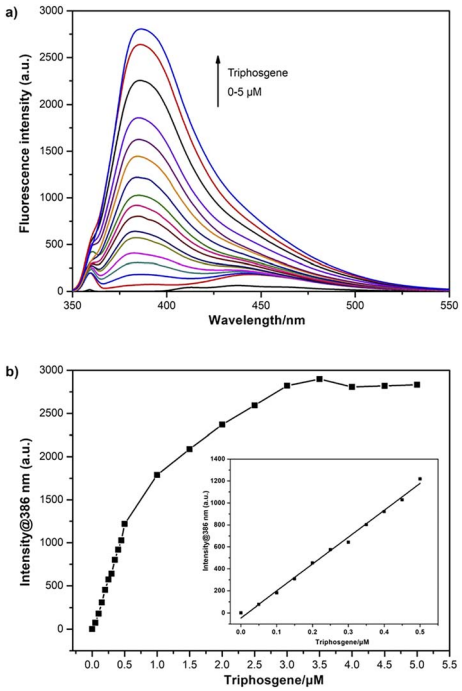

Fig. 3 (a) Fluorescence spectra of 10 μM **4-AHBI** upon addition of triphosgene (0–5 μM), λ_{ex} = 357 nm, slit width = 2.5/2.5 nm; (b) plot of the fluorescence intensity at 386 nm as a function of triphosgene (0–5 μM). Inset: linear correlation between fluorescence intensities at 386 nm and triphosgene (0–0.5 μM).

Table 1 Comparison of reported probes for triphosgene detection

Probes	Linear range (μM)	LoD (nM)	Ref.
Phos-2	0–3.6	0.2	10
Phos-4	0–14	1.9	11
RDM-670	0.6–1.5	0.42	12
Probe 1	0–2000	1150	13
4-AHBI	0–0.5	0.08	This work

Preparation of 4-AHBI loaded test papers and detection of triphosgene

Filter paper strips (0.5 × 2.5 cm) were dipped in the **4-AHBI** stock solution (1.0 mM), then removed and dried under air. The dip-dry process was repeated for 3 times. The completed dried strips were dipped in solutions of triphosgene (3.5 μM) and various analytes (50 μM) and then removed and dried under air. The fluorescent response to each analytes was imaged under 365 nm UV-light.

Results and discussion

Investigation of solvents

Initially, different organic solvents were utilized as the reaction medium to investigate the solvent effect on the response of **4-AHBI** to triphosgene. The organic solvents we chose and studied were CH_2Cl_2, $CHCl_3$, MeOH, EtOH, MeCN, acetone, ethyl acetate (EtOAc), dimethyl sulfoxide (DMSO) and *N*,*N*-dimethylform-amide (DMF). As depictured in Fig. 1 and S2,† in polar solvent (CH_2Cl_2, MeCN, acetone and EtOAc), **4-AHBI** exerted weak fluorescence emission at 424–450 nm and a new emission peak appeared at 386 nm with the addition of triphosgene. The most obvious fluorescence changes was found in CH_2Cl_2. In polar protic solvents (methanol and ethanol) and aprotic solvents (DMF and DMSO) as well as $CHCl_3$, the emission peaks of **4-AHBI** appeared at 377, 425, 444, 441 and 440 nm and no obvious changes were found with the addition of triphosgene. These results indicated that the fluorescence property of **4-AHBI** was greatly affected by the solvent[17] and further theoretical study of the solvation effect is undergoing in our group. Therefore, we chose CH_2Cl_2 as the solvent for the fluorescence detection of triphosgene.

Optical property

The optical properties of **4-AHBI** before/after addition of triphosgene were investigated by UV-vis absorption and fluorescence spectroscopy. As shown in Fig. 2, the maximum absorption and emission peaks of **4-AHBI** were located at 335 and 437 nm. Very low fluorescence quantum yields (Φf = 1.6%) was calculated with quinine sulphate as the reference (Φf = 54% in 1.0 M H_2SO_4) (Fig. S3†). With the addition of triphosgene, the absorption peak slightly red-shifted to 344 nm and obvious turn-on fluorescence emission was found at 386 nm. In addition, the nonfluorescent solution of **4-AHBI** changed to bright blue under the irradiation of 365 nm UV light (inset of Fig. 2).

Spectral response study

The fluorescence response characteristics of **4-AHBI** towards triphosgene was carried out. As shown in Fig. 3, when different concentrations of triphosgene (0–5 μM) were added, the fluorescence intensity of **4-AHBI** solution showed a regular increase at 386 nm with the maximum excitation at 357 nm. Excellent linear correlation between fluorescence intensities at 386 nm and triphosgene concentration was found over the range of 0–0.5 μM. The limit of detection (LoD) for triphosgene was determined to be 0.08 nM (LoD = $3\sigma/k$, where σ is the standard

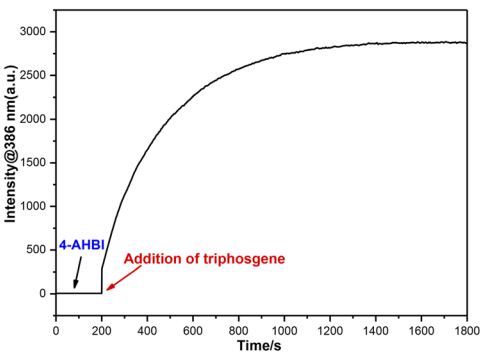

Fig. 4 Time-dependent fluorescence intensity at 386 nm of **4-AHBI** (10 μM) treated with triphosgene (3.5 μM), λ_{ex} = 357 nm, λ_{em} = 386 nm, slit width = 2.5/2.5 nm.

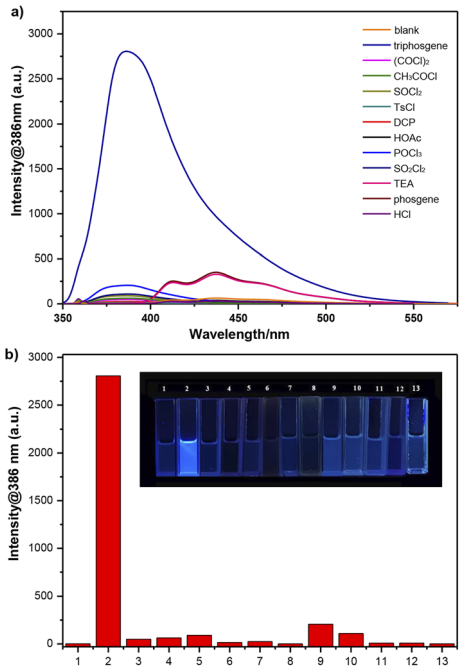

Fig. 5 (a) Fluorescence spectra and (b) fluorescence intensities at 386 nm of **4-AHBI** (10 μM) treated with triphosgene (3.5 μM) or various analytes (50 μM) for 30 min: (1) blank, (2) triphosgene (3.5 μM), (3) $(COCl)_2$, (4) CH_3COCl, (5) $SOCl_2$, (6) TsCl, (7) DCP, (8) HOAc, (9) $POCl_3$, (10) SO_2Cl_2, (11) TEA (20 μL, 0.1 mM in CH_2Cl_2), (12) phosgene (triphosgene (20 μL, 1.67 mM in CH_2Cl_2)/TEA (20 μL, 0.1 mM in CH_2Cl_2)), (13) HCl. λ_{ex} = 357 nm. Inset: photograph of these solutions under 365 nm UV-light.

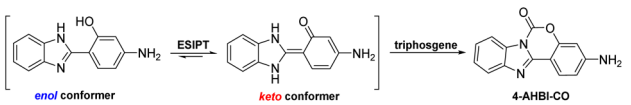

Scheme 2 Proposed mechanism of the interaction between **4-AHBI** and triphosgene.

deviation of the blank experiment, and k is the slope of the relationship between the intensity and the triphosgene concentration (Fig. S4†).

A comparison of this probe with published works for the detection of triphosgene is listed in Table 1. It can be seen that a wide range of LoD has been reported and **4-AHBI** in this work showed an acceptable detection limit. This result indicated that **4-AHBI** could be potentially employed as an optical sensor for the quantitative analysis of triphosgene in solution.

Response time

In order to evaluate the response time of **4-AHBI** to triphosgene, the time-dependent fluorescence spectra were performed. As displayed in Fig. 4, the fluorescence intensity at 386 nm for **4-AHBI** (10 μM) with 3.5 μM triphosgene were recorded. As it can be seen, after the addition of triphosgene, the fluorescence intensity increased rapidly in 2 minutes and reached the maximum within 20 minutes.

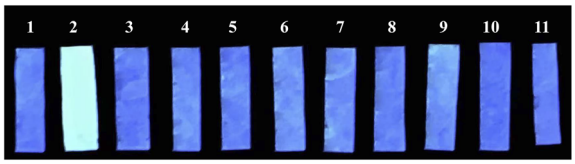

Fig. 6 Photographic images of **4-AHBI** loaded test papers upon dipped in solutions of triphosgene (3.5 μM) or various analytes (50 μM): (1) blank, (2) triphosgene (3.5 μM), (3) $(COCl)_2$, (4) CH_3COCl, (5) $SOCl_2$, (6) TsCl, (7) DCP, (8) HOAc, (9) $POCl_3$, (10) SO_2Cl_2, (11) HCl, under 365 nm UV-light.

Sensing selectivity

The selectivity of **4-AHBI** for the detection of triphosgene over potential interferents were assessed. As shown in Fig. 5, various competitive analytes including $(COCl)_2$, CH_3COCl, $SOCl_2$, *p*-toluenesulfonyl chloride (TsCl), diethyl chlorophosphate (DCP), glacial acetic acid (HOAc), phosphorus oxychloride ($POCl_3$), sulfonyl chloride (SO_2Cl_2), triethylamine (TEA), phosgene and HCl, were added to the **4-AHBI** solution under the same experimental conditions. Distinct changes in the fluorescence spectra of **4-AHBI** solution was induced by triphosgene, compared to negligible changes by the other analytes including phosgene. Furthermore, the determination of triphosgene in the presence of these interfering compounds were performed. As shown in Fig. S5 and Table S1,† the fluorescent intensities at 386 nm were not significantly affected by interfering compounds at 5.0 μM and good recovery rates were obtained (77.1–111.4%).

Mechanism study

Based on previously reported literature[15,18] and our investigations, a plausible sensing mechanism is proposed as depictured in Scheme 2. In CH_2Cl_2, **4-AHBI** shows one main fluorescence emission band at 437 nm with a Stokes shift 6967 cm^{-1} (>5834 cm^{-1}), which indicates the existence of ESIPT process and the major keto conformer of **4-AHBI** in solution. With the addition of triphosgene, the –OH and imidazole –NH of **4-AHBI** are connected by the carbonyl group, resulting to a block of the ESIPT process. The blue-shifted fluorescent emission could be attributed to the 'enol' conformer of **4-AHBI**. In order to confirm the proposed mechanism, the reaction mixture was analysed by HPLC-MS and the sensing product was synthesized and characterised by ^1H NMR and HRMS. As depictured in Fig. S6–8,† the dominant sensing product with a molecular weight of

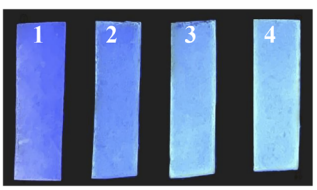

Fig. 7 Photographic images of **4-AHBI** loaded test papers upon dipped in solutions of triphosgene. (1): 0 μM, (2): 0.5 μM, (3): 1.0 μM and (4): 1.5 μM.

252.0776 should be **4-AHBI-CO** ($C_{14}H_{10}N_3O_2$ $[M + H]^+$: calculated 252.0768). These data strongly backed the proposed mechanism.

Practical strips detection

In order to develop practical applications, simple **4-AHBI** loaded test paper strips were prepared and used for the detection of triphosgene. As shown in Fig. 6, test strips exhibited non-fluorescence under 365 nm UV light. After treated with triphosgene, an obvious turn-on fluorescence emission was clearly observed compared to non-changes with other analytes. More importantly, **4-AHBI** loaded test strips were also effective for low concentrations of triphosgene (Fig. 7).

Conclusion

In summary, we have designed and synthesized a new 2-(2′-hydroxyphenyl)benzimidazole derived probe (**4-AHBI**) by introducing an amino group at the C4′ position. This probe displayed high selectivity towards triphosgene over other acyl chlorides including phosgene and sensitivity with a low LoD (0.08 nM) over the range of 0–0.5 μM. Moreover, practical **4-AHBI** loaded test strips were fabricated and applied to sense triphosgene with an easily observed turn-on fluorescence emission. With these exciting results, we believe that this probe would be of great importance for further development of selective and sensitive sensors for triphosgene.

Author contributions

Wen-Zhu Bi and Yang Geng: conceptualization, analysis, writing – review & editing. Wen-Jie Zhang, Chen-Yu Li and Chu-Sen Ni: methodology, formal analysis, investigation, visualization. Qiu-Juan Ma and Su-Xiang Feng: writing – review & editing, validation. Xiao-Lan Chen and Ling-Bo Qu: validation, supervision.

Conflicts of interest

There are no conflicts to declare.

Acknowledgements

This work was supported by Zhongjing Scholars Research Funding of Henan University of Chinese Medicine (No. 00104311-2023-21).

Notes and references

1 (*a*) A. Ghorbani-Choghamarani and G. Azadi, *Curr. Org. Chem.*, 2016, **20**, 2881; (*b*) M. O. Ganiu, B. Nepal, J. P. V. Houten and R. Kartika, *Tetrahedron*, 2020, **76**, 131553; (*c*) A. C. Chaskar, S. Yewale, R. Bhagat and B. P. Langi, *Synth. Commun.*, 2008, **38**, 1972; (*d*) W. Su, W. Zhong, G. Bian, X. Shi and J. Zhang, *Org. Prep. Proced. Int.*, 2004, **36**, 499; (*e*) S. Huang, B. Yan, S. Wang and X. Ma, *Chem. Soc. Rev.*, 2015, **44**, 3079.

2 For selected examples see: (*a*) Z. Li, Z. Jiang, Q. Shao, J. Qin, Q. Shu, W. Lu and W. Su, *J. Org. Chem.*, 2018, **83**, 6423; (*b*) A. H. Cleveland, F. R. Fronczek and R. Kartika, *J. Org. Chem.*, 2018, **83**, 3367; (*c*) X. He, S. Majumder, J. Wu, C. Jin, S. Guo, Z. Guo and M. Yang, *Org. Chem. Front.*, 2019, **6**, 2435; (*d*) Q. Xing, J. Zhao, Y. Zhu, X. Hou and Y. Wang, *Res. Chem. Intermed.*, 2023, **49**, 241.

3 L. Cotarca, T. Geller and J. Répási, *Org. Process Res. Dev.*, 2017, **21**, 1439.

4 (*a*) Y. Kong, T. Sun, M. Yu and H. Xia, *Anal. Bioanal. Chem.*, 2022, **414**, 4953; (*b*) W. Li, F. Liu, C. Wang, H. Truebel and J. Pauluhn, *Toxicol. Sci.*, 2012, **131**, 612; (*c*) W. W. Holmes, B. M. Keyser, D. C. Paradiso, R. Ray, D. K. Andres, B. J. Benton, C. C. Rothwell, H. M. Hoard-Fruchey, J. F. Dillman, A. M. Sciuto and D. R. Anderson, *Toxicol. Lett.*, 2016, **244**, 8; (*d*) S. Saha and P. Sahoo, *Environ. Sci.: Processes Impacts*, 2023, **25**, 1144; (*e*) C. Cao, L. Zhang and J. Shen, *Front. Immunol.*, 2022, **13**, 917395.

5 (*a*) L. J. Priestley, F. E. Critchfield, N. H. Ketcham and J. D. Cavender, *Anal. Chem.*, 1965, **37**, 70; (*b*) G. G. Esposito, D. Lillian, G. E. Podolak and R. M. Tuggle, *Anal. Chem.*, 1977, **49**, 1774; (*c*) M. Palit, D. Pardasani, A. K. Gupta and D. K. Dubey, *Anal. Chem.*, 2005, **77**, 711.

6 (*a*) H. B. Singh, D. Lillian and A. Appleby, *Anal. Chem.*, 1975, **47**, 860; (*b*) S. Qureshi, M. Asif, H. Sajid, M. A. Gilani, K. Ayub, M. Arshad and T. Mahmood, *Mater. Sci. Semicond. Process.*, 2022, **148**, 106753.

7 (*a*) L. Chen, D. Wu and J. Yoon, *ACS Sens.*, 2018, **3**, 27; (*b*) N. Kwon, Y. Hu and J. Yoon, *ACS Omega*, 2018, **3**, 13731; (*c*) X. Liu, N. Li, M. Li, H. Chen, N. Zhang, Y. Wang and K. Zheng, *Coord. Chem. Rev.*, 2020, **404**, 213109; (*d*) J. Tan, Z. Li, Z. Lu, R. Chang, Z. Sun and J. You, *Dyes Pigm.*, 2021, **193**, 109540; (*e*) X. Hu, Y. Ke, H. Ye, B. Zhu, J. Rodrigues and R. Sheng, *Dyes Pigm.*, 2023, **216**, 111379; (*f*) B. Zhu, R. Sheng, T. Chen, J. Rodrigues, Q. Song, X. Hu and L. Zeng, *Coord. Chem. Rev.*, 2022, **463**, 214527.

8 For selected examples see: (*a*) Y. Hu, L. Chen, H. Jung, Y. Zeng, S. Lee, K. M. Swamy, X. Zhou, M. H. Kim and J. Yoon, *ACS Appl. Mater. Interfaces*, 2016, **8**, 22246; (*b*) X. Zhou, Y. Zeng, C. Liyan, X. Wu and J. Yoon, *Angew. Chem., Int. Ed.*, 2016, **55**, 4729; (*c*) Y. Hu, X. Zhou, H. Jung, S. J. Nam, M. H. Kim and J. Yoon, *Anal. Chem.*, 2018, **90**, 3382; (*d*) Q. Hu, C. Duan, J. Wu, D. Su, L. Zeng and R. Sheng, *Anal. Chem.*, 2018, **90**, 8686; (*e*) L. Yang, Z. Sun, Z. Li, X. Kong, F. Wang, X. Liu, J. Tang, M. Ping and J. You, *Anal. Methods*, 2019, **11**, 4600; (*f*) X. Miao, W. Feng and Q. Song, *Dyes Pigm.*, 2023, **216**, 111348; (*g*) K. Liu, M. Qin, Q. Shi, G. Wang, J. Zhang, N. Ding, H. Xi, T. Liu, J. Kong and Y. Fang, *Anal. Chem.*, 2022, **94**, 11151; (*h*) Y. Li, J. Zhang, Z. Liang, R. Yang, L. Qu, Z. Li and Y. Sun, *Sens. Actuators, B*, 2023, **376**, 132971; (*i*) J. Zhang, Y. Li, J. Hu, Y. Sun, R. Yang, Z. Li and L. Qu, *Chem. Eng. J.*, 2023, **452**, 139173; (*j*) L. Zeng, T. Chen, B. Zhu, S. Koo, Y. Tang, W. Lin, T. D. James and J. S. Kim, *Chem. Sci.*, 2022, **13**, 4523.

9 For selected examples see: (*a*) S. Wang, L. Zhong and Q. Song, *Chem. Commun.*, 2017, **53**, 1530; (*b*) T. Kim, B. Hwang, J. Bouffard and Y. Kim, *Anal. Chem.*, 2017, **89**,

12837; (*c*) W. Zhang, K. Cheng, X. Yang, Q. Y. Li, H. Zhang, Z. Ma, H. Lu, H. Wu and X. Wang, *Org. Chem. Front.*, 2017, **4**, 1719; (*d*) H. Xia, X. Xu and Q. Song, *ACS Sens.*, 2017, **2**, 178; (*e*) W. Feng, S. Gong, E. Zhou, X. Yin and G. Feng, *Anal. Chim. Acta*, 2018, **1029**, 97; (*f*) L. Zeng, H. Zeng, L. Jiang, S. Wang, J. T. Hou and J. Yoon, *Anal. Chem.*, 2019, **91**, 12070; (*g*) A. Gangopadhyay, S. S. Ali and A. K. Mahapatra, *ChemistrySelect*, 2019, **4**, 8968; (*h*) X. Wei, Y. Fu, M. Xue and Q. Song, *Org. Lett.*, 2019, **21**, 9497; (*i*) H. Li, H. Xia, F. Nie and Q. Song, *J. Org. Chem.*, 2021, **86**, 8308; (*j*) Y. Huang, W. Ye, Y. Su, Z. Wu and H. Zheng, *Dyes Pigm.*, 2020, **173**, 107854; (*k*) S. Wang, B. Zhu, B. Wang, P. Fan, Y. Jiu, M. Zhang, L. Jiang and J. Hou, *Dyes Pigm.*, 2020, **173**, 107933.

10 S. Wang, L. Zhong and Q. Song, *Chem. - Eur. J.*, 2018, **24**, 5652.

11 S. Wang, C. Li and Q. Song, *Anal. Chem.*, 2019, **91**, 5690.

12 H. Chu, Q. Xie, X. Zhao, Z. Xu, S. Geng, C. Liu, X. Zhou, L. Yang, W. Han and J. Zhou, *Sens. Actuators, B*, 2022, **371**, 132557.

13 N. Jain and N. Kaur, *J. Fluoresc.*, 2023, DOI: **10.1007/s10895-023-03328-7**.

14 Z. Li, W. Zhang, W. Bi, Q. Ma, S. Feng, X. Chen and L. Qu, *RSC Adv.*, 2021, **11**, 10836.

15 Y. Yang, Y. Ding, W. Shi, F. Ma and Y. Li, *J. Lumin.*, 2020, **218**, 116836.

16 E. Barni, P. Savarino, M. Marzona and M. Piva, *J. Heterocycl. Chem.*, 1983, **20**, 1517.

17 (*a*) Y. Yang, Z. Tang, P. Zhou, Y. Qi, Y. Wang and H. Wang, *J. Mol. Liq.*, 2018, **260**, 447; (*b*) H. Xu, Y. Yu, L. Chen, Y. Feng, H. Xuan and H. He, *Comput. Theor. Chem.*, 2023, **1224**, 114104; (*c*) Y. Qi, M. Lu, Y. Wang, Z. Tang, Z. Gao, J. Tian, X. Fei, Y. Li and J. Liu, *Org. Chem. Front.*, 2019, **6**, 3136; (*d*) H. Zhang, W. Li, Y. Wang, Y. Tao, Y. Wang, F. Yang and Z. Gao, *RSC Adv.*, 2021, **11**, 25795.

18 (*a*) S. Santra and S. K. Dogra, *Chem. Phys.*, 1998, **226**, 285; (*b*) F. S. Rodembusch, F. P. Leusin, L. F. Campo and V. Stefani, *J. Lumin.*, 2007, **126**, 728; (*c*) N. Dey, *ChemistrySelect*, 2020, **5**, 6823; (*d*) F. S. Rodembusch, F. P. Leusin, L. B. Bordignon, M. R. Gallas and V. Stefani, *J. Photochem. Photobiol., A*, 2005, **173**, 81.